

PERFORMANCE OF THE PWC  
CLUSTER LOGIC TRIGGER IN LASS \*

J. Va'vra<sup>†</sup>  
Carleton University  
Ottawa, Ontario, Canada K1S 5B6

S. Shapiro  
Stanford Linear Accelerator Center  
Stanford University, Stanford, California 94305

ABSTRACT

The performance of the cluster logic circuit used in the LASS Spectrometer is discussed. The intention of this paper is to familiarize users of the spectrometer with the properties of this device for forming multiplicity type triggers with any of the proportional chambers in LASS. A  $K^-p$  experiment (E-132) is used as an example.

(Submitted for Publication)

---

\* Work supported in part by Department of Energy, under contract number EY-76-C-03-0515.

<sup>†</sup> Work supported in part by Institute of Particle Physics of Canada, Toronto, Ontario, Canada M5S 1A7.

## Introduction

Historically, it has been desirable to use proportional wire chambers to form multiplicity type triggers for physics experiments, where multiplicity here refers to the number of particles passing through the chamber. It is well documented that one particle can give rise to more than one wire of the PWC having a measurable signal. Therefore a scheme must be developed to cluster groups of wires corresponding to the same particle and then to combine these clustered signals so that these may be used for the experimental trigger.

The cluster logic circuit used to form the PWC trigger has been incorporated into the initial design of the readout system and has been discussed previously.<sup>1</sup> Until recently, however, it had never been tested or used under experimental conditions. The purpose of this note is to share our experiences in using this circuit to generate a clean experimental trigger during the December, 1977 E-132 run at LASS.<sup>2</sup>

The primary thrust of E-132 is a high statistics study of  $K^-p$  interactions including final states having high mass, high spin and/or high decay multiplicity. The LASS spectrometer shown schematically in fig. 1 is ideally suited to these studies, as it has nearly  $4\pi$  solid angle acceptance and permits a measurement of the recoil baryon.

To obtain information on the many states of interest, a nonrestrictive trigger was designed. Initially it was thought sufficient to trigger on an identified beam particle ( $K^-$ ) and the requirement of two or more particles in the TOF hodoscope situated downstream of the  $\check{C}_1$  Cerenkov counter. This resulted in a trigger rate of 10.7%. Further

study revealed that triggers were included in the above rate caused by the decay or interaction of the  $K^-$  downstream of the target. Furthermore, a noninteracting  $K^-$  could produce a delta ray in passing through the material within the solenoid. This delta ray would then spiral downstream to the TOF hodoscope and cause a trigger.

The obvious solution to this problem was to place the requirement of two or more particles in the event as close to the downstream end of the target as possible. Figure 1 shows a full bore proportional chamber (named 1.5) 54 cm downstream of the target. It has three sense planes oriented horizontally, vertically, and at  $45^\circ$  to the horizontal (x,y,e). The sense wires are spaced 2 mm apart and cover an area of roughly 1.280 meters square.<sup>3</sup>

To use this proportional chamber in the trigger, we rely on the proper performance of the so called cluster logic circuit shown in fig. 2. The output of each hit wire feeds a signal to the gated cluster chain. The gating allows only signals from the highest numbered wire per cluster (group of consecutive hit wires) to contribute to the sum on the cluster bus. The analog signal on this bus is now proportional to the number of clusters hit within one chamber plane. This output is then, in principle, fed into a commercial discriminator where decisions as to multiplicity can be made based on this pulse height.

The real world imposes a series of roadblocks to using this sort of device. Proportional chambers have inherent time jitter associated with the drift of the electrons to the sense wires. Further time

jitter is caused by the variance of the pulse height of the initial PWC signals and the response of the amplifier/discriminator system chosen to detect them. A third effect which causes a time "walk" occurs later in the electronics where the time to threshold varies in the commercial discriminator as a function of the number of clusters involved in the event. Lastly, of course, the many crates of electronics involved will cause slight differences in the pulse height of the final signals and will have a slightly differing response to the electronic noise abounding in the system. All of these effects must be studied and understood before trusting this device to select our physics events.

The two basic types of testing to be done before use of this device involve using a pulse generator to simulate the PWC signals and later tests with a beam and the actual PWC inputs. Both are essential and are described fully in what follows.

#### Pulser Tests

a) The initial tests with the pulser allow us to detect dead channels in the cluster circuit. The digital readout which records the chamber performance will only serve to check out that part of the circuit prior to the analog addition viz. the amplifier/discriminator/shaper sections. To check the analog portion we must use pulser and scope.

b) The pulser tests allow us to equalize the pulse height from various crates. The system at present comprises 1280 channels set in five crates of electronics. While pulse height variations between

cards within a given crate are not significant, crate to crate variations were noticed and were eliminated by properly terminating the cluster logic bus.

c) These tests allow us to observe the electrical noise on the cluster logic lines generated by the digital readout clocks. When the noise was observed to be significant, (+90 mV to -40 mV peak to peak) we filtered the input to the final discriminator. The final value of noise after filtering is +70 mV to -20 mV peak to peak, oscillating with a roughly 200 nsec period. This noise value is to be compared to the -150 mV signal generated by a single cluster ( $\approx$  300 mV for doubles). The splitter/filter shown in fig. 2 was employed to achieve this reduction.

d) The pulser tests allow us to determine some basic timing characteristics of the circuit. Namely, we can measure the time walk caused by the final leading edge discriminator's response to cluster signals of varying pulse heights. The resultant time walk is shown in table I to be a 16 nsec difference between multiplicity 2 and multiplicity 8 events for a discrimination setting of 175 mV. Figure 3 demonstrates this feature as well as the magnitude of the signals per cluster - roughly 150 mV/cluster. The response of the circuit was measured to be linear for up to 8 clusters or 1.2 volts.

e) Finally, the pulser test allowed us to determine visually the effect on pulse height of out of time pulses. The results are shown in fig. 4. As mentioned above, the pulses from a PWC having an anode wire to wire spacing of 2 mm will have a time jitter of about 25 nsec. We observe that for a discriminator threshold of 175 mV we begin to lose efficiency if the relative delay between the two pulses is in excess of 32 nsec.

### Beam Tests

For further understanding of the circuit, we must now use the full system. The beam tests employed an rf separated 11 GeV  $K^-$  beam having 1-3 kaons per SLAC pulse. A one meter long liquid hydrogen target was also used. The major concerns regarding this circuit will be elaborated upon here:

a) To demonstrate the existence of a stable operating point for selecting events having multiplicities of two or greater per event, we must plot the appropriate plateau curve. This is a first indication of proper circuit performance. Figure 5 demonstrates the existence of adequately wide plateaus. Figure 5c is an overall discriminator curve showing plateaus for multiplicities as high as three. The extra effort necessary to observe plateaus for higher multiplicities separately was not expended. However, fig. 6 demonstrates the effects of raising the discriminator threshold level beyond 175 mv. The thresholds in these multiplicity curves are clearly moving to higher multiplicity with increasing discriminator threshold. Figures 5a and 5b demonstrate with a bit more clarity the plateau available for triggering on "more than one" or "more than two" particles/event.

b) The measured delay curve is shown in fig. 7. The fall off of events at large positive delays is evidence for the PWC jitter being on the order of 25 nsec. The width of the curve coupled with a knowledge of the maximum time walk expected for large multiplicities (determined in the pulser tests) confirms our choice of 60 nsec for the output cluster signal width as being reasonable.

c) The success of our circuit in eliminating events with zero or one particle in the event and in retaining events having two or more particles is examined next. Figure 8 demonstrates the former, confirming that the rejection efficiency for either the x or the y plane is nearly perfect. The top half of the figure shows the software multiplicity distribution for a trigger which does not require the cluster criterion. The bottom half is the same trigger with the cluster criterion added.

To discuss the efficiency for retaining events having two or more particles, we made use of a data sample wherein we did not demand the cluster logic cut. We did, however, record the existence of a cluster  $\geq 2$  signal. We could then compare the hardware trigger rate to one generated by having the software look at chamber 1.5 and demanding two or more hits. The two rates agreed to within the statistical accuracy of the test. As evidence for this see fig. 9. It is worth noting here that in order to eliminate any dependence of the trigger rate on the efficiency of the proportional chamber, we have taken the logical 'or' of the multiplicity in the x and y planes. If either shows two or more particles we trigger.

d) Software studies of trigger rates for E-132 suggested that the cluster logic not be active within the beam region. This was implemented by removing a 32 mm region from the center of both the x and y readouts (in the cluster circuit only). By comparing the first two columns of fig. 9 we see the reduction in trigger rate caused by this exclusion.

e) Our final trigger

$$T_{\phi} = BT \cdot TOF \geq 1 \cdot \left[ 1.5 x \geq 2 \text{ or } 1.5 y \geq 2 \right] \cdot \overline{LP}_3$$

resulted in a trigger rate of 6.8%.<sup>4</sup> We might ask whether our rate would be further reduced by applying a further cut, for instance, excluding events having more than eight particles. Table II shows the correlation matrix between our time of flight (TOF) hodoscope and the 1.5x plane multiplicities. That a strong correlation exists is evident. The improvement in the trigger rate due to excluding high multiplicity events is shown. The small reduction doesn't seem to warrant the effort necessary to implement this cut in E-132.

f) We have studied the contribution of the cluster logic to the random trigger rate and found that even though our  $CL_{\geq 2}$  signal was 60 nsec wide, randoms only increased the trigger rate by 2% of the prompt rate. This measurement was made at  $2K^-/\text{pulse}$ .

#### Alarms

The cluster circuit is a part of our trigger. If it fails, one would want to be aware of it immediately. To this end we considered the possible failure modes of the circuit and concluded that they would all result in the D.C. level of the cluster bus departing from its -5V value. A single alarm circuit sensing this level was implemented. If the level changes, a loud alarm awakens the physicist to the fact and turns off the experiment. The alarm sensor circuit is shown in fig. 10.

#### Conclusion

In conclusion, it is clear that this sort of circuitry is useful in eliminating useless events from our experiment. Our trigger rate was reduced from 10.8% to 6.8% resulting in a decrease of more than 60% in



the amount of data that now need not be analyzed. The details presented in this note will hopefully be useful to users of the LASS spectrometer in choosing the design of future experiments.<sup>5</sup>

REFERENCES

1. S. L. Shapiro, M. G. D. Gilchriese and D. G. McShurley, "A Proportional Chamber Front End Amplifier and Pulse Shaping Circuit". Stanford Linear Accelerator preprint SLAC-PUB-1713 (February 1976).
2. George Luste, "The Solenoid Vertex Spectrometer -- a Simulation Study", Stanford Linear Accelerator Center report SLAC-152 (June 1972). D. W. G. S. Leith, et al., "Study of Events with Direct  $e^+e^-$  Pairs in Hadron Collisions at 10 and 16 GeV/c", Stanford Linear Accelerator Center proposal for experiment, SLAC Exp. E-127 (August 1976). D. W. G. S. Leith, et al., "A Study of  $K^+p$  Interactions Using LASS", Stanford Linear Accelerator Center proposal for experiment, SLAC Exp. E-132.
3. Al Kilert, M. G. D. Gilchriese, S. L. Shapiro, "The Mechanical Design and Construction of a 12,000 Wire Proportional Chamber System for LASS", Stanford Linear Accelerator Center (1979) (to be published).
4. The implementation of the cluster logic allowed us, in this case, to loosen the multiplicity requirement on the TOF counters. This resulted in the added benefit of increasing our mass acceptance.
5. C. Y. Chein, et al., Stanford Linear Accelerator Center experiment number E-129, has investigated using the cluster logic trigger on the cylindrical PWC chamber surrounding the target. In an attempt to increase the percentage of events having a slow recoil proton, the PWC voltage was lowered, and one or more hits from the cylinder cluster logic demanded in the trigger. The results were encouraging.

TABLE I

## TIME WALK MEASUREMENT

Multiplicity	Delay (nsec)
2	0
3	9
4	11
5	13
6	15
7	16
8	16

Discriminator Threshold Set at 175 mVolt.

TABLE II

## TOF-Cluster Correlation Matrix

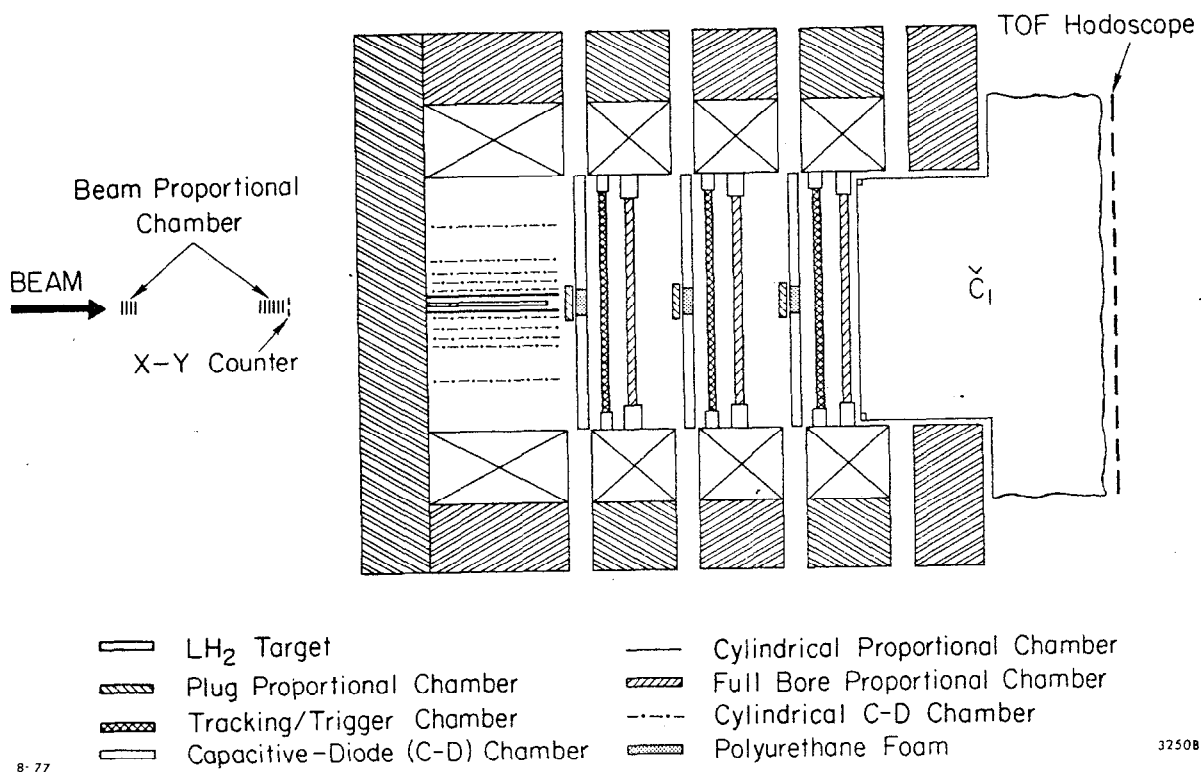
TOF Multiplicity	PWC Multiplicity (1.5x)										
	0	1	2	3	4	5	6	7	8	9	$\geq 10$
0	1	0	0	0	0	0	0	0	0	0	0
1	72	36	18	9	0	3	0	1	0	0	0
2	448	336	238	145	63	34	18	8	5	1	3
3	235	153	234	201	162	84	18	21	6	3	4
4	138	93	115	191	118	99	56	32	14	10	10
5	72	54	61	91	123	94	60	44	17	7	15
6	48	24	29	49	63	71	60	36	18	11	11
7	27	21	20	19	36	36	27	22	15	11	16
8	19	7	6	12	8	20	22	25	14	7	18
9	3	5	3	4	9	12	13	12	7	9	0
$\geq 10$	10	9	6	10	27	22	26	31	18	23	60

The trigger for the above study was  $BT \cdot TOF \geq 2 \cdot \overline{LP3}$ . Cutting at PWC  $\geq 8$  would reduce the trigger  $BT \cdot TOF \geq 2 \cdot \overline{LP3} \cdot \{1.5 \times \geq 2\}$  by a further 10%.

FIGURE CAPTIONS

1. LASS solenoid instrumentation.
2. The cluster logic circuit.
3. Pulse shape of the analog signal for one through four cluster.
4. Pulse height versus the delay between two PWC signals as determined in pulser tests.
5. Cluster discrimination curves
  - a) The  $T_0$  trigger "doubles" plateau
  - b) The  $T_2$  "singles" plateau
  - c) The overall discrimination curve
6. Multiplicity curves for various discriminator threshold settings.
7. The delay curve at the  $T_0$  coincidence: the pulse width of the  $CL \geq 2$  signal is 60 nsec, the pulse width of the BT signal is 7 nsec. The  $T_0$  trigger is  $BT \cdot TOF \geq 2 \cdot \{(1.5 x \geq 2) \text{ or } (1.5 y \geq 2)\}$ , the bracketed quantity is the  $CL \geq 2$  signal. The curve has been normalized to BT. The maximum time walk indicated is that determined from pulser tests for very large cluster multiplicities.
8. Comparison of resultant multiplicity distributions with and without the cluster cut in the trigger.
9. Trigger comparisons.
  - a) Software simulation of the  $T_0$  cluster cut without the  $\pm 16$ mm hole.
  - b) Software simulation of the  $T_0$  cluster cut with the  $\pm 16$ mm hole.
  - c) The hardware  $T_0$  cluster cut with the  $\pm 16$ mm hole
  - d) The  $T_0$  trigger with no cuts.

10. a) The cluster circuit alarm sensor mounted on each crate of electronics.
- b) The alarm receiver mounted in a NIM module.



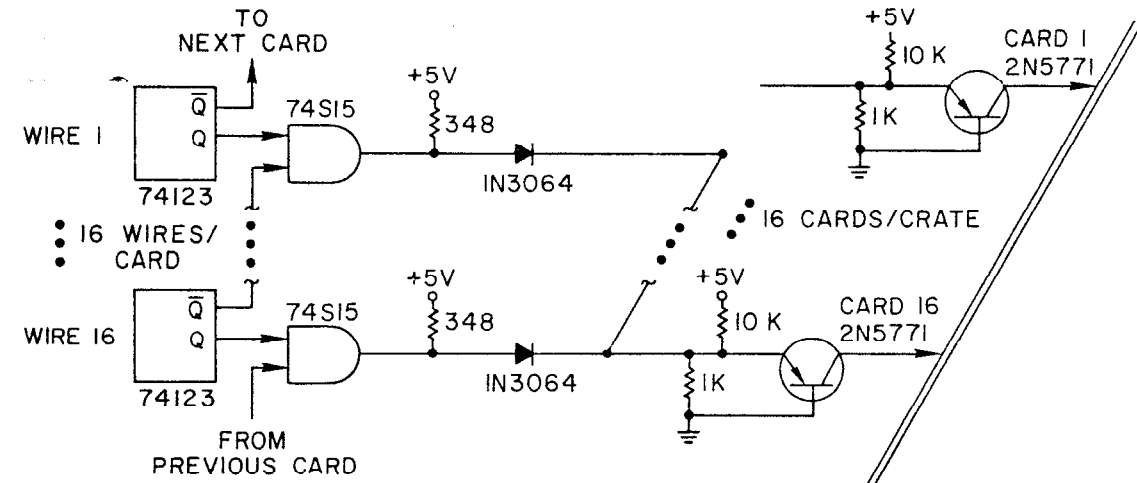
8-77

3250B1

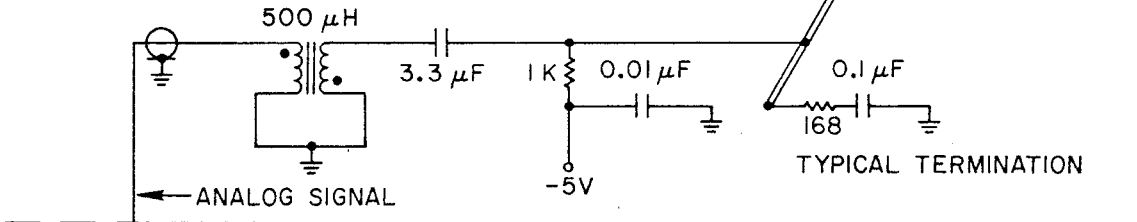
Fig. 1

# CLUSTER LOGIC CIRCUIT

LOGIC IN ONE 16 WIRE CARD:



## CLUSTER DETECTOR (ONE/CRATE)



## FINAL CLUSTER LOGIC (E-132)

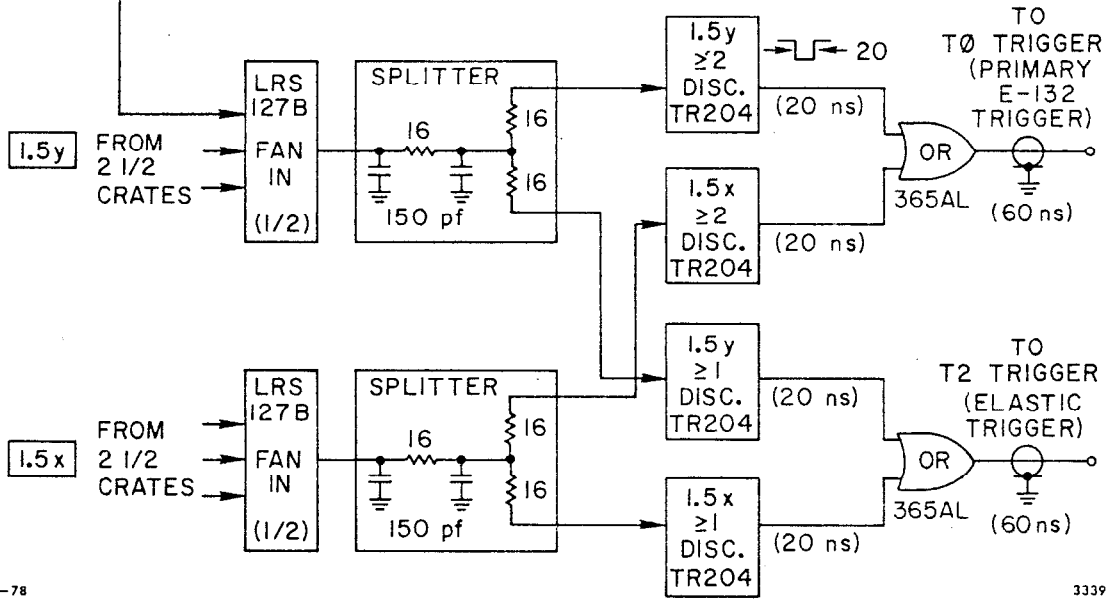


Fig. 2



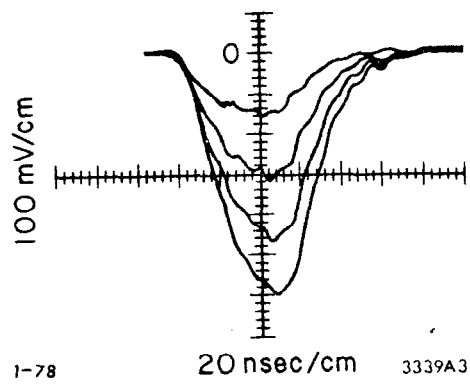
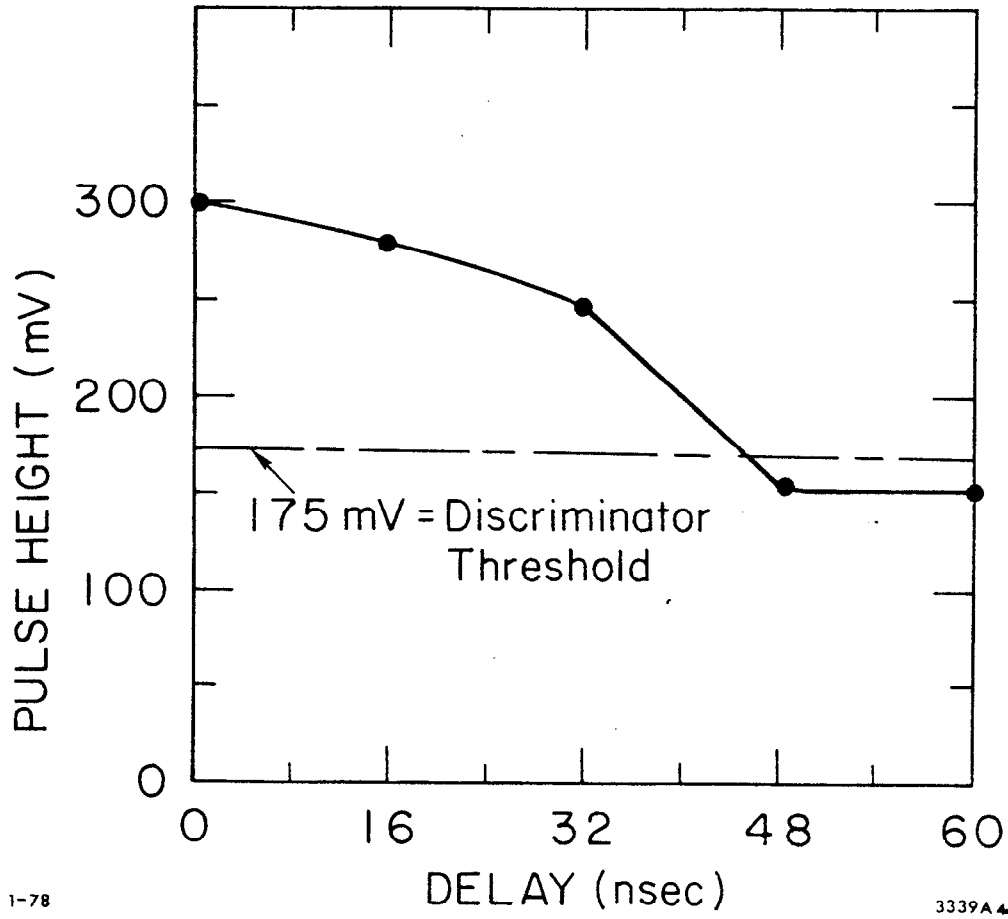


Fig. 3



1-78

3339A4

Fig. 4

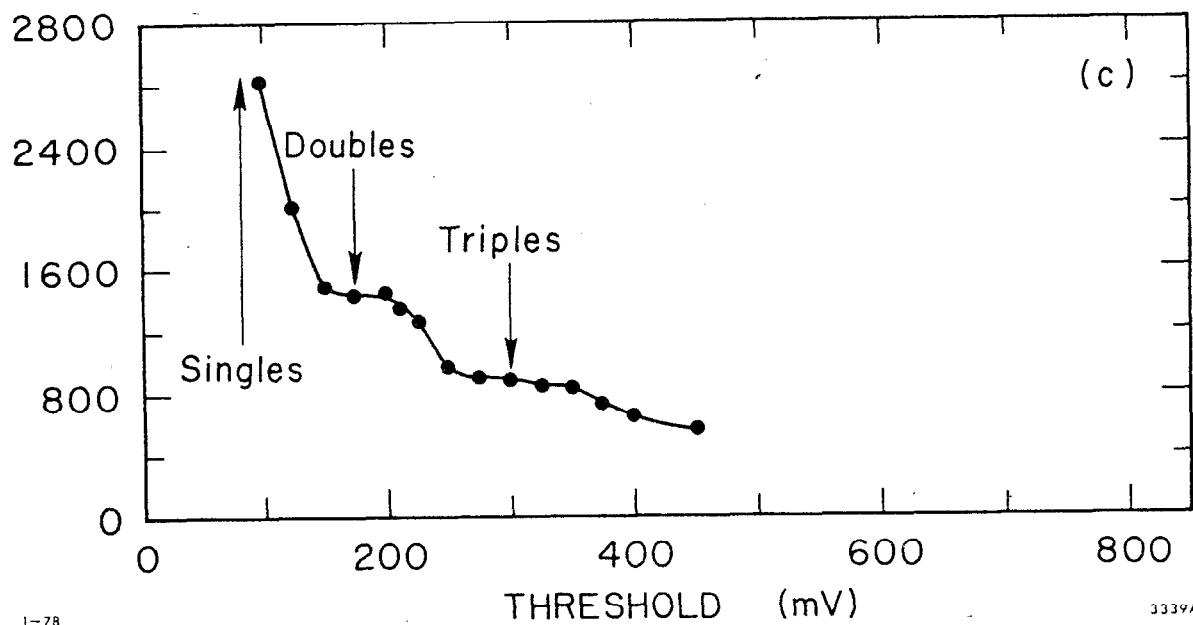
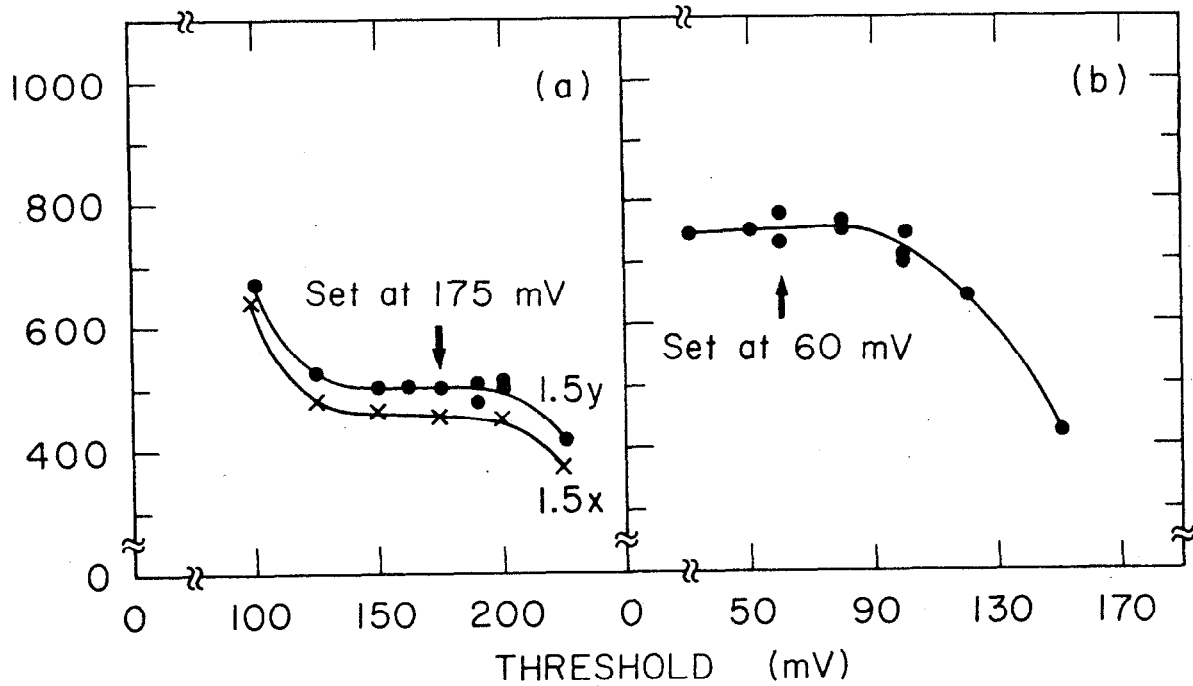


Fig. 5

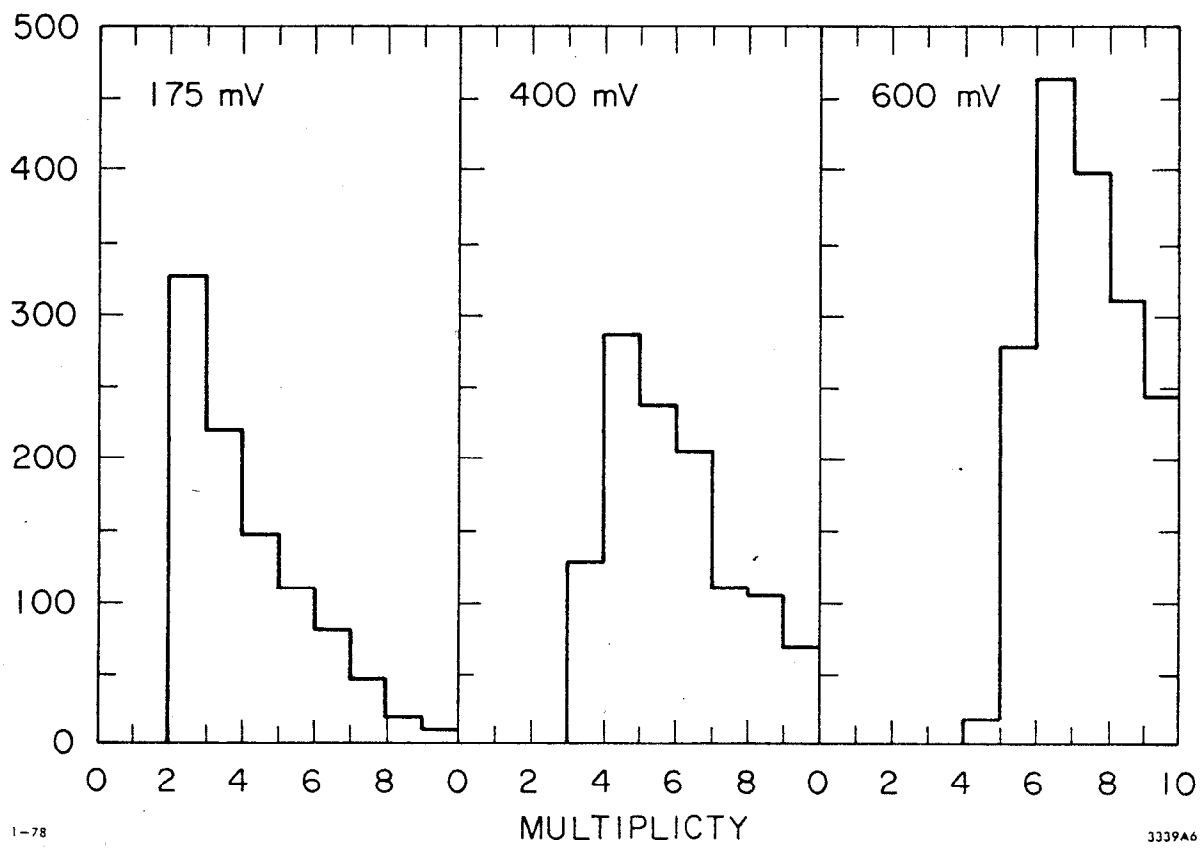


Fig. 6

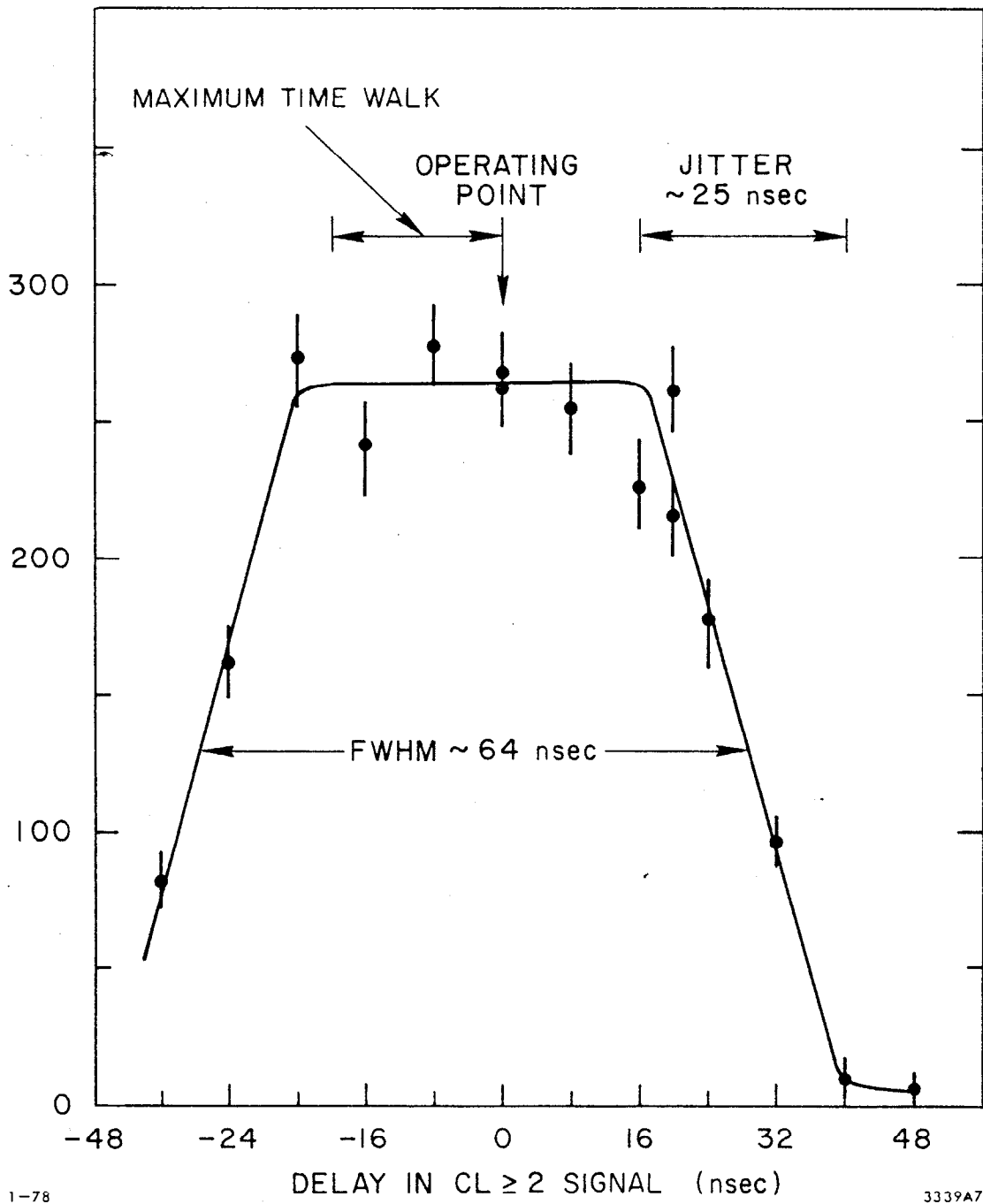


Fig. 7

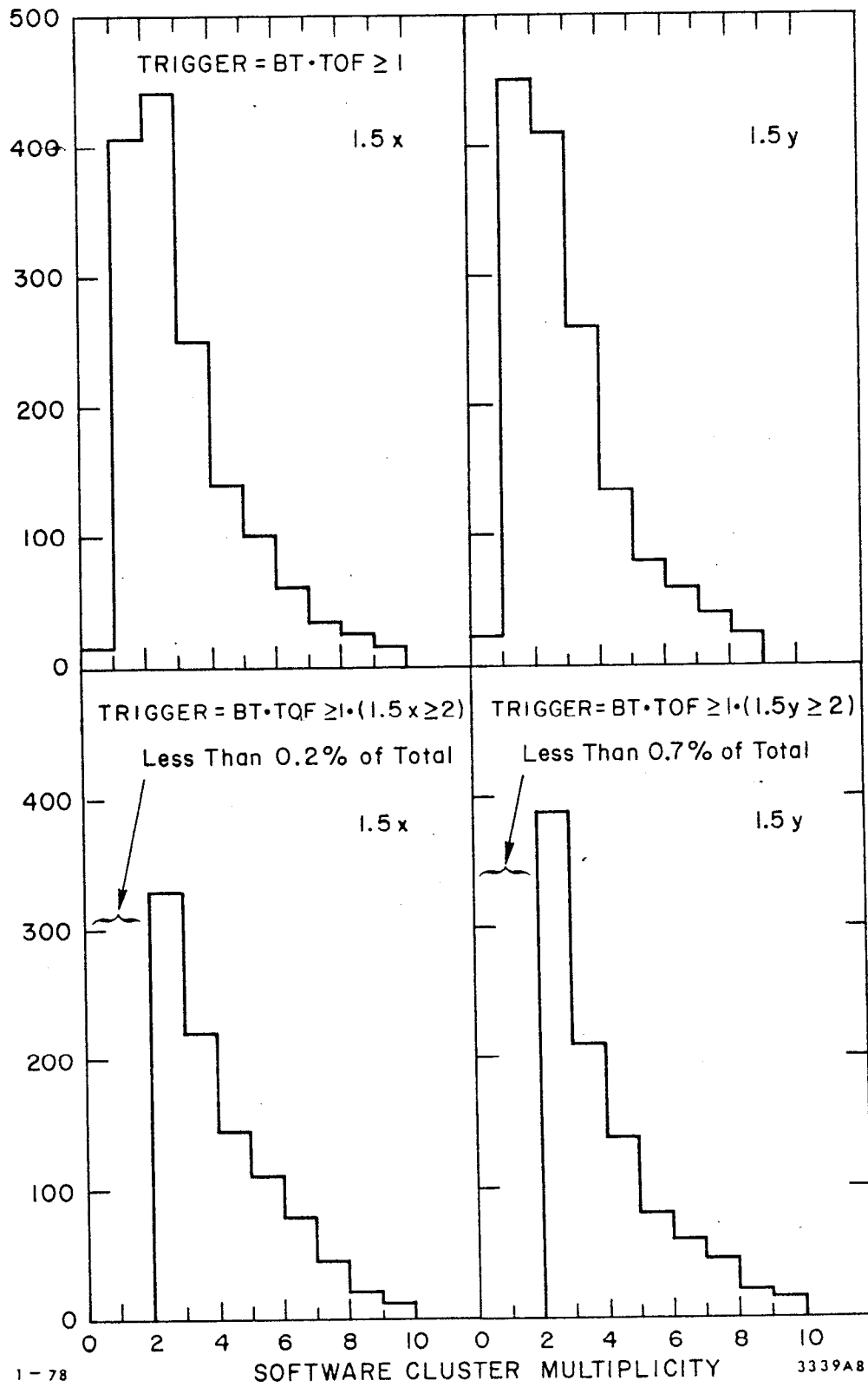


Fig. 8

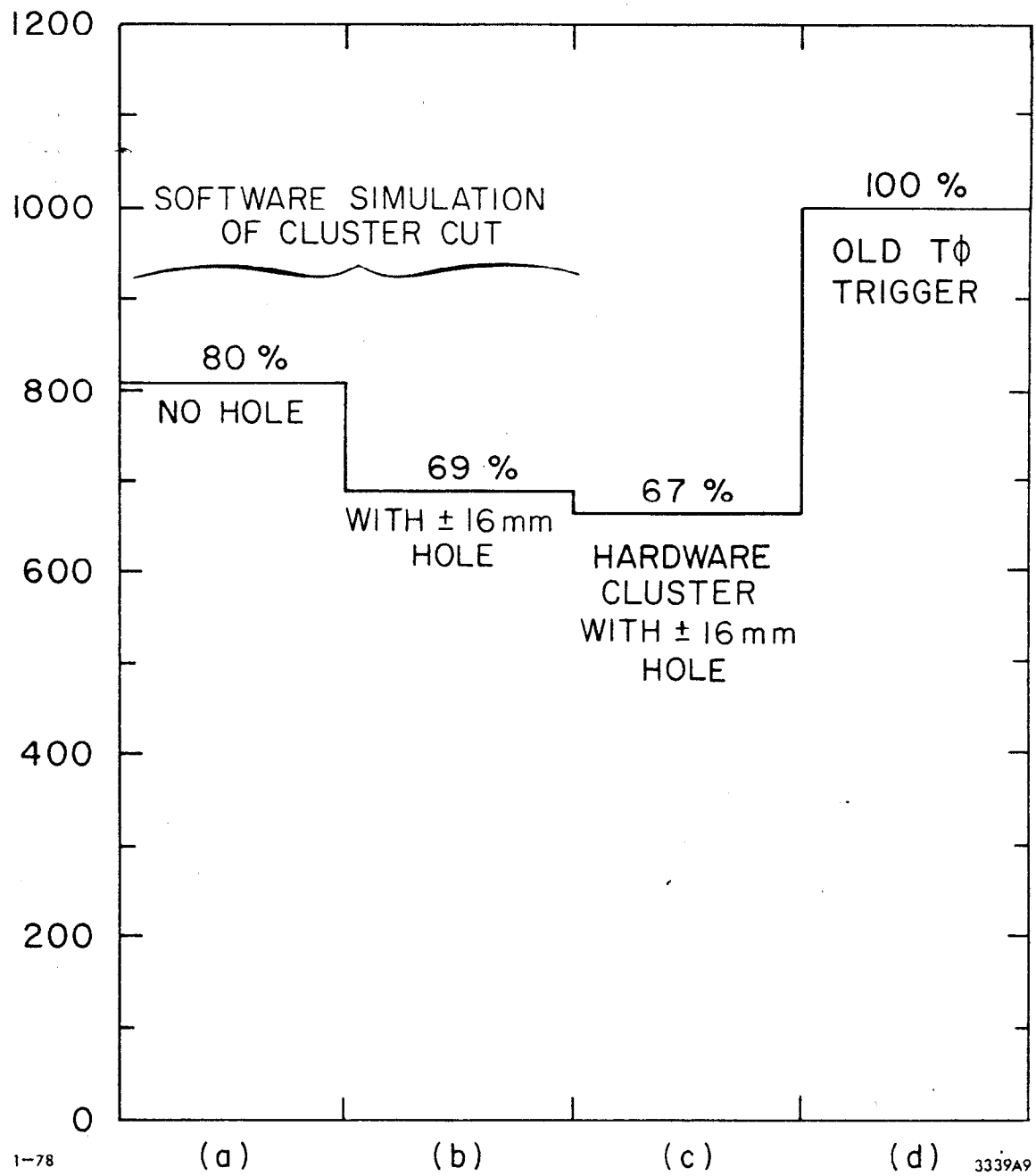
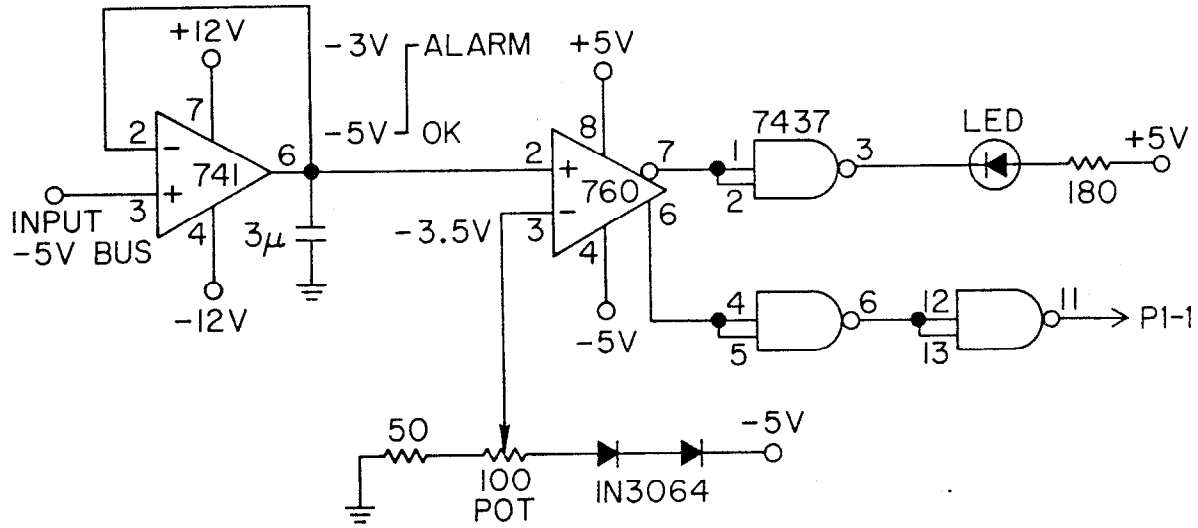
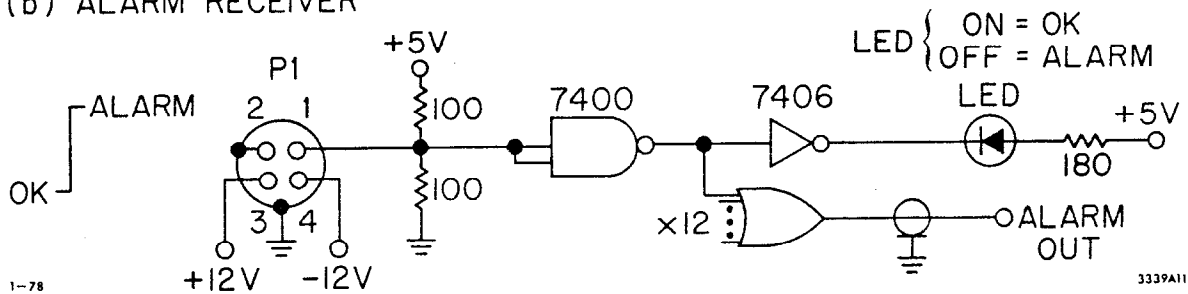


Fig. 9

(a) ALARM SENSOR



(b) ALARM RECEIVER



1-78

3339A11

Fig. 10